CDF/PUB/BOTTOM/PUBLIC/3609

Version 1.0

Ratios of b Quark Fragmentation Probabilities and Bottom Meson Branching Fractions Involving J/ψ Mesons

CDF Collaboration

(March 15, 1996)

Abstract

We report a measurement of the b quark fragmentation probabilities f_u, f_d and f_s and ratios of branching fractions of the B^+, B^0 and B_s^0 mesons into exclusive final states containing a J/ψ meson. The final states were selected from 19 pb^{-1} of $p\bar{p}$ collisions recorded by the Collider Detector at Fermilab. We also determine the branching fractions for the decay modes $B^+ \to J/\psi K^+$, $B^+ \to J/\psi K^*(892)^+$, $B^0 \to J/\psi K^0$, $B^0 \to J/\psi K^*(892)^0$ and $B_s^0 \to J/\psi \phi(1020)$. This is the first reported measurement of this B_s^0 branching fraction. We discuss the implications of these measurements to B meson decay models.

13.25.Hw, 13.87.Fh, 14.40.Nd

I. INTRODUCTION

The bound states of heavy quarks provide a laboratory in which we can investigate the behaviour of the strong force (Quantum Chromodynamics or QCD) and the electroweak interaction [1]. The lowest-lying bound states are the pseudoscalar mesons with one bottom anti-quark bound to one of the three lightest quarks, the B^+, B^0, and B_s^0 mesons. The branching fractions ($\mathcal{B}$) of these mesons into final states consisting of only hadrons (the fully hadronic decays) have been studied theoretically and have been shown to yield insights into the complex interactions that take place between a quark and anti-quark pair at short distance scales [2–4].

Experimental studies of bottom meson hadronic decays have been limited by their relatively small branching fractions (typically 10^{-2} to 10^{-3}) and the difficulty of detecting the final states. The most precise branching fraction measurements have been made at e^+e^- colliders, where the B^+ and B^0 mesons are pair-produced at threshold [5,6]. Bottom hadrons are produced copiously in high-energy proton-antiproton collisions [7–9], and so it is possible to measure the branching fractions of bottom mesons into those fully hadronic final states that have unique final state topologies. We report a study of the branching fractions of bottom mesons into final states consisting of a J/ψ meson and a light quark meson, using the Collider Detector at Fermilab (CDF). The data come from a 19.6 pb^{-1} run of the Fermilab Tevatron Collider producing 1.8 TeV proton-antiproton collisions. This work extends an earlier analysis of the same dataset [10] by incorporating an additional final state, $J/\psi\phi(1020)$, estimating the fragmentation fractions of B hadrons, and providing improved measurements of the branching fractions of B^+ and B^0 mesons. We use the convention that the charge-conjugate state is implied whenever we refer to a specific charge state or decay mode.

We have focused our study on the bottom meson decay modes that yield a J/ψ meson that subsequently decays to a $\mu^+\mu^-$ final state. This results in a signature that we can readily identify using the CDF trigger system and provides the necessary rejection of other background processes. We have measured the observed production cross section times branching fraction for the following channels:

$$B^+ \to J/\psi K^+, \tag{1}$$

$$B^0 \to J/\psi K^0, \tag{2}$$

$$B^+ \to J/\psi K^*(892)^+, \tag{3}$$

$$B^0 \to J/\psi K^*(892)^0, \tag{4}$$

$$B_s^0 \to J/\psi \phi(1020). \tag{5}$$

The cross section for the decay mode $B^+ \to J/\psi K^+$ can be decomposed into the form

$$\sigma_{\rm obs} = \sigma(p\bar{p} \to \bar{b}) f_u \mathcal{B}(B^+ \to J/\psi K^+)\epsilon^{K^+}, \tag{6}$$

and similar forms can be written for the other decays. Here, ϵ^{K^+} is the efficiency of detecting the $J/\psi K^+$ final state, $\sigma(p\bar{p} \to \bar{b})$ is the bottom quark production cross section and f_u is the probability that the fragmentation of a b anti-quark will result in a B^+ meson. In a similar way, we define f_d and f_s to be the probabilities of a b anti-quark to hadronize and form a B^0 and B_s^0 meson, respectively. We will refer to these probabilities as fragmentation fractions, and explicitly include in this fraction contributions from decays of heavier B hadrons into final states containing a B^+, B^0 or B_s^0 meson.

The fragmentation fractions into the different B meson states are largely unmeasured. If one assumes that this fraction is independent of the flavor and energy of the quark initiating the hadronization process, then measurements of strange meson production in jet fragmentation provide the most accurate estimates of f_s [11]. Only one measurement of f_s in the B meson system exists [12], and this has large uncertainties. No measurements have been made of f_u or f_d in the B meson system, despite the importance of these in many B hadron branching fraction, lifetime and mixing studies [13].

The bottom meson production cross section $\sigma(p\bar{p} \to \bar{b})$ is not precisely known; the best measurements to date have uncertainties of order $\pm 20\%$ [9]. The efficiency of detecting the final state, ϵ^{K^+}, depends on an understanding of the b quark production properties and detector acceptance. We therefore present our measurements in the form of ratios of branching fractions in order to avoid introducing additional uncertainties due to the b quark production cross section and the final state detection efficiency. We then compare these ratios directly with phenomenological predictions of the relative B meson branching fractions. We also use our data to estimate the fragmentation fractions f_u, f_d and f_s.

We have organised this report as follows. In Section II, we describe the data selection and procedures that we followed to reconstruct the five decay modes. We present in Section III a study of the relative size of resonant and non-resonant $K\pi$ and KK final states to the B meson decays. We describe the procedure used to determine the acceptance and efficiency corrections for each decay mode in Section IV. In Section V, we present the results of this study and conclude in Section VI.

II. DATA COLLECTION AND SELECTION

CDF is a multi-purpose detector designed to study high-energy $p\bar{p}$ collisions produced by the Fermilab Tevatron Collider. It surrounds the $p\bar{p}$ interaction point with three charged particle tracking detectors immersed in a 1.4 T solenoidal magnetic field. The tracking system is contained within a hermetic calorimeter system that measures the energy flow of charged and neutral particles. Charged particle detectors outside the calorimeter are used to identify muon candidates.

The innermost tracking device is a silicon microstrip detector (SVX) located in the region between 3.0 and 7.9 cm in radius from the beam axis [14]. This is followed by a set of time projection chambers (VTX) that measure charged particle trajectories out to a radius of 22 cm. An 84-layer drift chamber (CTC) measures the particle trajectories in the region between 30 and 130 cm in radius from the beam. This tracking system has high efficiency for detecting charged particles with transverse momentum $P_T > 0.35$ GeV/c, and the CTC and SVX together measure charged particle transverse momenta with a precision of $\sigma_{P_T} \sim [(0.0066 P_T)^2 + (0.0009 P_T^2)^2]^{1/2}$ (with P_T in units of GeV/c).

The muon detection system consists of 4 layers of planar drift chambers separated from the interaction point by 5-9 interaction lengths of material. An additional 4 layers of chambers is located outside the magnet return flux in the central pseudorapidity region $|\eta| < 0.7$ to reduce the probability of misidentifying penetrating hadrons as muon candidates. An additional set of chambers are located in the pseudorapidity interval $0.7 < |\eta| < 1.0$ to extend the acceptance of the muon system. The muon system is capable of detecting muons with $P_T \gtrsim 1.4$ GeV/c in a pseudorapidity interval $|\eta| < 1.0$. These and other elements of the CDF detector are described in more detail elsewhere [15].

We selected the J/ψ final states using a three-level trigger system that identified collisions that produced two muon candidates. The first level trigger required that there be two track candidates observed in the muon system. The level one trigger efficiency rises from $\sim 40\%$ at $P_T = 1.5$ GeV/c to $\sim 93\%$ for muons with $P_T > 3$ GeV/c. The second level trigger requires the detection of a charged track in the CTC using the Central Fast Track processor (CFT), which performs a partial reconstruction of all charged tracks above a momentum of ~ 2.5 GeV/c in the axial view. The CTC track is required to match within 15^0 of the muon candidate. The CFT efficiency rises from 40% at a muon $P_T = 2.6$ GeV/c to $\sim 94\%$ for $P_T > 3.1$ GeV/c. The third level trigger requires that two reconstructed CTC tracks match with two muon track segments and that the dimuon invariant mass be between 2.8 and 3.4 GeV/c^2. The efficiency of the level three trigger requirement is $97 \pm 2\%$ for J/ψ candidates that pass the dimuon selection used in this analysis. Approximately 2.06×10^5 dimuon candidate events passed the level three trigger requirements.

These events were further selected to identify a clean sample of J/ψ candidates. We required that each muon candidate have a high-quality CTC track candidate with $P_T > 1.4$ GeV/c that, when extrapolated to the muon chambers, matched within 3 standard deviations of the extrapolation and measurement uncertainties with a muon track stub in the transverse plane $(r - \phi)$ and along the beam axis direction (z). The two muon candidates were required to have opposite signs. We performed a least-squares fit of the two muon candidate tracks under the constraint that the two tracks come from a common point (a vertex constraint).

We required the probability of this fit to be greater than 0.01. These requirements resulted in a signal of $(7.89 \pm 0.08) \times 10^4$ J/ψ decays on a background of non-resonant dimuon candidate events. The dimuon invariant mass distribution for this sample is shown in Fig. 1, along with an estimate of the background determined using same-sign muon candidate pairs. We performed an additional fit to the dimuon system, applying a vertex constraint and requiring that the dimuon invariant mass equal the world average J/ψ mass of 3.09688 GeV/c^2 [13]. The confidence level of this fit was required to be greater than 0.01.

We reconstructed the exclusive decay modes listed in Eqs. 1-5 by forming charged particle combinations with the J/ψ candidate. For the decay channel $B^+ \rightarrow J/\psi K^+$, we required the K^+ candidate to have $P_T > 1.5$ GeV/c and the resulting B^+ candidate to have $P_T > 8.0$ GeV/c. A least-squares fit was performed on the three charged tracks forming the $J/\psi K^+$ candidate by constraining the three tracks to come from a common vertex, the invariant mass of the dimuon system to equal the world average J/ψ mass, and the flight path of the B^+ candidate to be parallel to its momentum vector in the transverse plane (a 2-dimensional pointing constraint). The confidence level of this least-squares fit had to exceed 0.01. We required the fitted transverse momenta of the muon candidate with lowest and highest P_T to be greater than 1.8 and 2.5 GeV/c, respectively. This ensured that the muon candidates were likely to pass the dimuon trigger requirements. In order to reduce the backgrounds from prompt J/ψ production, we required the B^+ meson candidate flight path to be pointing in the same hemisphere as its momentum vector (in effect requiring the B^+ candidate proper decay length, $c\tau$, to be positive). The $J/\psi K^+$ invariant mass distribution is shown in Fig. 2a). We have performed a binned maximum likelihood fit of this data to a Gaussian lineshape and a linear background term and estimate a B^+ signal of 154 ± 19 events. The width of the signal was not constrained in the fit and resulted in a fitted mass resolution of 0.015 ± 0.002 GeV/c^2, consistent with our expected detector resolution.

The reconstruction of the other four decay modes was performed with similar criteria in order to reduce the systematic uncertainties resulting from the kinematics of the produced B mesons and selection biases. Identical requirements were made on the quality and transverse momenta of the muon candidates, constraints on the fits to the B decay topologies, B meson lifetimes and K_s^0 lifetimes. We allowed for small variations in the B and light quark meson transverse momentum requirements to optimise the expected significance for each channel. The significance is defined as $S/\sqrt{S+B}$, where S is the expected number of events determined using a Monte Carlo calculation for a given integrated luminosity, and B is the extrapolated background rate under the signal region using the observed B meson sideband background levels. This resulted in only modest differences in the P_T requirements from channel to channel, and did not introduce significant systematic uncertainties in our estimation of the B meson detection efficiency.

The decay mode $B^0 \to J/\psi K^0$ was reconstructed by searching for $K^0 \to K_s^0 \to \pi^+\pi^-$ candidates using all pairs of oppositely-signed charged particles that formed a secondary vertex. The daughter pions were required to have $P_T > 0.4$ GeV/c. To fully reconstruct the $B^0 \to J/\psi K_s^0$ decay, we performed a least-squares fit to the two pion candidate tracks and two muon candidates, constraining each track pair to come from common points, requiring the momentum vector of the K_s^0 candidate to point along its flight path (a vertex and pointing constraint) and placing K_s^0 and J/ψ mass constraints on the dipion and dimuon systems, respectively. The confidence level of the fit had to exceed 0.01. To improve the signal-to-noise ratio, we required the proper decay length ($c\tau$) of the K_s^0 candidate to be larger than 0.1 cm and that its transverse momentum be greater than 1.5 GeV/c. The $\pi^+\pi^-$ invariant mass distribution for the K_s^0 candidates that satisfy these requirements is illustrated in Fig. 3a), and shows a K_s^0 signal of $(2.56 \pm 0.05) \times 10^4$ decays above a large combinatorial background (for illustration, no mass constraints were imposed in the least-squares fit to the charged tracks in this figure). To identify a clean B^0 candidate sample, we required the $J/\psi K_s^0$ candidates to have $P_T > 6.0$ GeV/c, and we required them to have a $c\tau$ greater than zero to reduce the combinatorial backgrounds from prompt J/ψ production. This selection resulted in a signal of 36.9 ± 7.3 B^0 decays. The invariant $J/\psi K_s^0$ mass distribution for these candidates is shown in Fig. 2b).

We searched for the decay mode $B^+ \to J/\psi K^*(892)^+ \to J/\psi K_s^0\pi^+$ by selecting a sample of J/ψ candidate events containing a K_s^0 candidate. The criteria used to identify K_s^0 candidates for the $J\psi K_s^0$ final state were also used for this decay mode. We required the K_s^0 candidates to have $P_T > 2.0$ GeV/c. We considered all other charged tracks with $P_T > 0.4$ GeV/c as π^+ candidates and we combined these with the K_s^0 candidates to form all possible $K^*(892)^+ \to K_s^0\pi^+$ candidates. The combinatorial backgrounds to the $K^*(892)^+$ decay are large. The $K_s^0\pi^+$ invariant mass distribution is presented in Fig. 3c). A fit to this distribution results in an estimated $K^*(892)^+$ signal of $(1.8 \pm 0.5) \times 10^3$ decays. In order to identify a B^+ candidate sample, a least-squares fit similar to that imposed on the $J/\psi K_s^0$ candidates was performed. We required that the confidence level of this fit be greater than 0.01, and that the $c\tau$ of the K_s^0 candidate be greater than 0.1 cm. The transverse momentum of the B^+ candidate had to exceed 6.0 GeV/c and its $c\tau$ had to be positive. In order to isolate a $K^*(892)^+$ resonance, we required that the invariant $K_s^0\pi^+$ mass be within 0.08 GeV/c^2 of the world average $K^*(892)^+$ mass (0.8916 GeV/c^2) [13]. This results in the $J/\psi K_s^0\pi^+$ invariant mass distribution shown in Fig. 2c). A signal of 12.9 ± 4.3 candidate events is observed.

Our data selection to reconstruct the decay $B^0 \to J/\psi K^*(892)^0 \to J/\psi K^+\pi^-$ proceeded in a similar manner. We formed combinations of all oppositely-charged track pairs, and fit the four charged tracks requiring that they come from a common decay point, constraining the invariant dimuon mass to the world average J/ψ mass, and requiring that the flight path of the B^0 candidate be parallel to its momentum vector in the transverse plane. The confidence level of this fit had to be greater than 0.01 and the B^0 candidate $c\tau$ had to be positive. The combinatorial backgrounds to the $K^*(892)^0$ decay are also large. This is illustrated in Fig. 3d), where we show the $K^+\pi^-$ invariant mass distribution for events that have transverse momentum of the $K^+\pi^-$ system greater than 2.0 GeV/c. We defined the B^0 candidate sample by requiring the P_T of the two-track system to be greater than 2.0 GeV/c and the resulting $J/\psi K^+\pi^-$ system to have $P_T > 8.0$ GeV/c. We required the $K^+\pi^-$ invariant mass to be within 0.08 GeV/c^2 of the world average $K^*(892)^0$ mass (0.8961 GeV/c^2). The resulting $J/\psi K^+\pi^-$ invariant mass distribution is shown in Fig. 2d).

This peak also has contributions from symmetric $K^*(892)^0$ decays where the incorrect kaon and pion mass assignments yield an invariant $K\pi$ mass within the K^{*0} mass window of ± 0.08 GeV/c^2. We used a Monte Carlo calculation to determine the relative fraction of such combinations and the shape of the resulting $J/\psi K^+\pi^-$ invariant mass distribution. The signal shape was parametrised by two Gaussian distributions with the normalization, position and width of the two functions determined by a fit to the $J/\psi K^+\pi^-$ invariant mass distribution predicted by a Monte Carlo calculation. This shape was then used in a fit to the observed $J/\psi K^*(892)^0$ invariant mass distribution to determine the number of B^0 decays in our data. This procedure yields a signal of 95.5 ± 14.3 $B^0 \rightarrow J/\psi K^*(892)^0$ decays. This assumes that the B^0 decays into this final state were only via the two-body $J/\psi K^*(892)^0$ intermediate state.

The search for the decay mode $B_s^0 \rightarrow J/\psi\phi(1020) \rightarrow J/\psi K^+K^-$ was performed by considering as $\phi(1020) \rightarrow K^+K^-$ candidates all oppositely-charged track pairs. A least-squares fit of the $\mu^+\mu^-K^+K^-$ candidate system was performed, constraining all four tracks to come from the same vertex, constraining the dimuon invariant mass to the world average J/ψ mass, and imposing a 2-dimensional pointing constraint on the B_s^0 decay. The confidence level of this fit had to exceed 0.01. A $\phi(1020)$ signal of $(4.1\pm0.4)\times10^3$ events is evident in this sample, as illustrated in Fig. 3b). The combinatorial background was reduced by requiring the K^+K^- system to have $P_T > 2.0$ GeV/c, the $J/\psi K^+K^-$ system to have $P_T > 6.0$ GeV/c and the $c\tau$ of the B_s^0 candidate system to be positive. We defined our $\phi(1020) \rightarrow K^+K^-$ candidate sample by requiring the K^+K^- invariant mass to be within 0.01 GeV/c^2 of the world average ϕ mass (1.0194 GeV/c^2) [13]. This resulted in a sample with the $J/\psi K^+K^-$ invariant mass distribution shown in Fig. 2e). A B_s^0 signal is evident on a relatively small background. A fit of this signal to a Gaussian lineshape results in an total signal of 29.4 ± 6.2 events.

III. RESONANT AND NON-RESONANT DECAYS

Clear signals for B meson production and decay are observed in all five channels. In the case of the three channels involving a strongly decaying resonance in the final state, the total number of B candidate events in principle results from resonant and non-resonant contributions in the final state. We searched for evidence of a non-resonant B contribution by placing invariant mass cuts on the B candidate and examining the $K_s^0\pi^-$, $K^+\pi^-$ and K^+K^- invariant mass distributions. In order to account for non-B background in the two-body mass distributions, we defined B mass sideband regions for the three samples, normalised to the estimated number of non-B events as determined from the B invariant mass distributions. The signal and sideband regions are described in Table I.

The $K_s^0\pi^+$, $K^+\pi^-$ and K^+K^- invariant mass distributions are illustrated in Fig. 4 for the B signal and sideband regions (the shaded distributions are from candidates in the sideband regions normalised to the background under the B meson peak in the signal region). One sees from these distributions resonant signals for the $K^*(892)$ and $\phi(1020)$ with no significant non-resonant contributions above the non-B backgrounds. We quantified the amount of resonance production associated with the B signals by performing binned maximum likelihood fits of the two-body invariant mass distributions to Breit-Wigner lineshapes convoluted with detector resolution, using the normalised sideband distributions to model the shape and size of the background under the resonance signal. The resulting numbers of observed events, N_{sb}, are listed in Table I. As a cross-check, we also estimated the number of signal events by fitting the resonance signals to Breit-Wigner lineshapes convoluted with detector resolution and background shapes described by second-order polynomial functions. The resulting event rates, N_{fit}, are listed in Table I and are consistent with N_{sb}.

Under the assumption that there are no non-resonant decays, we can also estimate the strength of the two-body resonant decay by correcting the observed B rates determined from the fits to the $J/\psi K\pi$ and $J/\psi KK$ invariant mass distributions for the loss in efficiency due to the $K\pi$ and KK mass cuts. The efficiencies have been estimated using a Monte Carlo calculation to be 0.80 and 0.86 for the $K\pi$ and KK mass window cuts, respectively. The resulting B meson rates, N_{win}, are also listed in Table I. We see no significant difference in rate due to these three methods. We therefore conclude that we do not observe a significant non-resonant $B \to J/\psi K\pi$ or $B_s^0 \to J/\psi KK$ decay mode. We choose N_{sb} as the best estimate of the rate of resonant production as it is least biased by potential contributions from non-resonant production.

IV. EFFICIENCY CORRECTIONS

We estimate the relative reconstruction efficiency for each B meson decay mode to convert the observed number of B events into ratios of branching fractions. We write the efficiencies for reconstructing B mesons as

$$\epsilon^{K^+} = \epsilon_{J/\psi} \times \epsilon_{geom}^{K^+} \times \epsilon_{c\tau}^{K^+} \times \epsilon_K \tag{7}$$

$$\epsilon^{K^0} = \epsilon_{J/\psi} \times \epsilon_{geom}^{K^0} \times \epsilon_{c\tau}^{K^0} \times \epsilon_{K_s} \tag{8}$$

$$\epsilon^{K^{*+}} = \epsilon_{J/\psi} \times \epsilon_{geom}^{K^{*+}} \times \epsilon_{c\tau}^{K^{*+}} \times \epsilon_{K_s} \times \epsilon_\pi \tag{9}$$

$$\epsilon^{K^{*0}} = \epsilon_{J/\psi} \times \epsilon_{geom}^{K^{*0}} \times \epsilon_{c\tau}^{K^{*0}} \times \epsilon_K \times \epsilon_\pi \tag{10}$$

$$\epsilon^{\phi} = \epsilon_{J/\psi} \times \epsilon_{geom}^{\phi} \times \epsilon_{c\tau}^{\phi} \times \epsilon_\phi, \tag{11}$$

where we show the common contributions. The quantity $\epsilon_{J/\psi}$ is the efficiency for triggering and reconstructing the $J/\psi \to \mu^+\mu^-$ decay and cancels for all decay modes. This also includes the combined efficiencies of the vertex and vertex-plus-mass constrained fits of 0.952 ± 0.006, which cancels out in our subsequent analysis. The quantities $\epsilon_{geom}^{(i)}$ are the geometrical efficiencies for finding the daughter mesons in the tracking fiducial volume, having the decay exceed the minimum P_T requirements on the meson and B systems given a J/ψ candidate, and having the B candidate satisfy the constrained fit requirements. The quantities $\epsilon_{c\tau}^{(i)}$ are the efficiencies of the proper decay length requirement on the B candidate in the different decay modes. The quantities ϵ_K, ϵ_{K_s}, ϵ_π and ϵ_ϕ are the efficiencies for reconstructing the K^+, K_s^0, π^- and ϕ mesons using the charged track information.

In addition to these efficiencies, we correct the observed event rates for the relevant branching fractions into intermediate states, $\mathcal{B}(K^0 \to K_s^0 \to \pi^+\pi^-) = 0.3430 \pm 0.0014$ and $\mathcal{B}(\phi(1020) \to K^+K^-) = 0.491 \pm 0.009$, both taken from Ref. [13], and the isospin weighting factors $\mathcal{B}(K^*(892)^0 \to K^+\pi^-) = \mathcal{B}(K^*(892)^+ \to K^0\pi^+) = 2/3$.

Since we are only interested in ratios of efficiencies, the common terms in these efficiencies cancel, reducing the overall uncertainties. These include the term $\epsilon_{J/\psi}$, and the reconstruction efficiencies ϵ_K or ϵ_{K_s} when they appear in both the numerator and denominator of the ratio. A number of other quantities do not necessarily cancel when calculating the ratio of branching fractions. In order to evaluate the relative efficiencies, we employed a B meson Monte Carlo calculation. B mesons were generated uniformly in the interval $|\eta| < 1.0$, with a P_T spectrum predicted by a next-to-leading order QCD calculation [16] using the MRS D0 proton structure functions [17]. The b quark P_T was required to be > 5 GeV/c, and the b quark fragmentation into a B meson was modeled using the Peterson parametrization with the parameter ϵ chosen to be 0.006 [18]. The B mesons were decayed using the CLEO B decay model [19] and a full simulation was used to model the response of the CDF detector, including effects due to the underlying event. The resulting Monte Carlo events were then processed with the same algorithms used to reconstruct the collider data. We then used these data to estimate the geometrical acceptances $\epsilon_{geom}^{(i)}$. These efficiencies are listed in Table II.

The geometrical efficiencies, $\epsilon_{geom}^{(i)}$, include the effect of the B meson vertex and mass constrained fits. We determined that the efficiency of the fitting procedure and subsequent confidence level requirements were independent of B decay mode by measuring the relative loss in signal events when different event topologies were fit employing both a vertex constraint and a vertex-plus-mass constraint. We assigned a systematic uncertainty of 1% in the relative acceptances to this effect. We also investigated the uncertainties associated with the model of the detector used to measure the reconstruction efficiencies. We verified that the detector simulations accurately described the interaction vertex distributions and detector geometry. We then compared the efficiencies determined using the complete detector simulation to those determined using a parametrised model of the detector. Based on this comparison, we conservatively assigned a 5% systematic uncertainty on the relative geometrical efficiencies to take into account any remaining uncertainties in the detector model.

In principle, the B meson $c\tau$ requirements have different efficiencies for each channel because of different momentum and vertex resolutions for the final states and possible differences in the lifetimes of the B meson states. We evaluated the efficiencies $\epsilon_{c\tau}^{(i)}$ using the world average values for the lifetimes of the three mesons [13], using vertex detector resolutions observed in the events in the B sideband regions. The results are listed in Table II. We repeated the efficiency calculation varying the lifetimes by one standard deviation. The resulting variations in the relative efficiencies were assigned as systematic uncertainties.

The meson reconstruction efficiencies take into account the charged track reconstruction efficiencies, the efficiencies of the K_s^0 lifetime cut and the additional constrained fits performed when a K_s^0 candidate is in the final state. The track reconstruction efficiencies were determined using both a full detector simulation and by imbedding simulated tracks in real interactions containing J/ψ candidates. The differences in the reconstruction efficiencies obtained in these ways were considered as systematic uncertainty in these efficiencies. The loss of $K^{\pm}$ mesons due to decays-in-flight was estimated using the full detector simulation. Between 4% and 6% of $K^{\pm}$ mesons decay within the volume of the CTC, of which approximately 40% are correctly reconstructed. We conservatively assigned a 3% systematic uncertainty on ϵ_K.

The K_s^0 lifetime cut efficiency and the efficiencies of the vertex and mass constrained fits were determined by measuring the loss of signal events in both the proper lifetime distribution and the $\pi^+\pi^-$ invariant mass distributions. The efficiency of the lifetime cut was determine to be 0.958 ± 0.007. The uncertainty represents the difference in efficiencies determined by estimating the loss of real K_s^0 decays using the $\pi^+\pi^-$ invariant mass and the $c\tau$ distributions for the candidate samples. The fractions of K_s^0 candidates that satisfied the confidence level requirements on the vertex and vertex-plus-mass constrained fits were

0.938 ± 0.013 and 0.983 ± 0.006, respectively.

A number of additional checks were made to verify that correlations in efficiencies were properly taken into account. The variation of the dimuon trigger acceptance for the different B meson final states was determined using a Monte Carlo calculation that simulated both the detector response and the effect of the trigger. This resulted in a negligible uncertainty in the ratio of acceptances. Variations in the P_T spectrum of the produced B mesons could also result in a change in the relative acceptance. This was measured by perturbing the renormalization scale and the b quark mass in the Monte Carlo calculation of this distribution. We assigned a systematic uncertainty on the relative acceptance due to this effect that varies from $1-5\%$, depending on the pair of final states being compared. The polarization of the vector mesons in the final state also has an effect on the relative acceptance. We varied the longitudinal polarization of the $K^*(892)$ meson by ± 0.10 around a nominal value of 0.75 and the $\phi(1020)$ meson longitudinal polarization by ± 0.25 around the nominal value of 0.50 [20]. We assigned the resulting 2.5% change in acceptance as the systematic uncertainty due to this effect.

We expect B^+, B^0 and B_s^0 mesons to be produced both directly and through the production of excited B meson states that decay to the pseudoscalar mesons we observe. We investigated the effect such resonant production would have on the relative ratio of efficiencies of the decay modes studied by performing a Monte Carlo calculation using the PYTHIA program [21], which models the production and resonant decay of higher mass B meson states. In this calculation, we assumed that the relative production of B mesons with orbital angular momentum L and spin S was in the ratio $0.30 : 0.53 : 0.17$ for $L = 1$ and $S = 0$ or 1: $L = 0$ and $S = 1$: $L = 0$ and $S = 0$. The change in the ratio of acceptances, relative to the case where only ground-state $({}^{2S+1}L ={}^1 0)$ meson production was assumed, varied from 1% to 4%, depending on the decay mode considered. We included this as an additional systematic uncertainty on the acceptance.

The systematic uncertainties assigned to the relative efficiencies are summarised in Table III. These were combined in quadrature to determine the total systematic uncertainty on the relative acceptance for each pair of decay modes used in this study.

V. RESULTS

We present our results as a matrix of ratios of branching fractions. The observed number of signal events, listed in Table II, were corrected by the relative detection efficiency for each decay to yield a production cross section times branching fraction for each channel. When we form the ten possible ratios of these acceptance-corrected event rates, the production cross section and the common efficiencies cancel. The results are listed in Table IV. Three of these ratios have also been determined using a different technique based on the same data set [10]. The values determined here are in good agreement with these previous results. Note that these two sets of measurements are not statistically independent.

The measured quantities are the ratios of the product of b quark fragmentation fractions into the different B meson species and the B meson branching fractions into the specific final state. Each of the ten ratios can be written in the form given by the following example:

$$R^{\phi}_{K^+} = \frac{f_s \mathcal{B}(B^0_s \to J/\psi\phi)}{f_u \mathcal{B}(B^+ \to J/\psi K^+)}. \qquad (12)$$

We can therefore use these data to constrain both the fragmentation fractions and the meson branching fractions.

A. Branching Fractions

The ratios of branching fractions that involve the B^0_s meson can be used with the world average values for the B^+ and B^0 meson branching fractions into the four other final states [13] to estimate the product of the ratio of fragmentation fractions, $f_s/(f_u, f_d)$, times the branching fraction $\mathcal{B}(B^0_s \to J/\psi\phi)$. The world average B^+ and B^0 branching fractions have been measured assuming that the fragmentation fractions f_u and f_d are equal for b quarks produced in $\Upsilon(4S)$ decays, and so this assumption is implicit in this calculation.

All ratios that involve the B^0_s can be rewritten in the form given by the example

$$f_s \mathcal{B}(B_s^0 \to J/\psi\phi) = f_u \mathcal{B}(B^+ \to J/\psi K^+) R_{K^+}^{\phi}, \tag{13}$$

which gives us four independent measures of the ratio of fragmentation fractions and the B_s^0 branching fraction, using the world average values for the branching fractions [13] on the right-hand side of Eq. 13. With the assumption of equal B^+ and B^0 fragmentation fractions, we form the weighted average of the four estimates to obtain

$$\frac{f_s}{(f_u, f_d)} \mathcal{B}(B_s^0 \to J/\psi\phi) = (0.37 \pm 0.11 \pm 0.04) \times 10^{-3}. \tag{14}$$

The two uncertainties are the statistical and systematic uncertainties, respectively.

In order to extract $\mathcal{B}(B_s^0 \to J/\psi\phi)$, we have assumed $f_u = f_d$ and $f_s = (0.40 \pm 0.06)\ f_u$. This value of f_s represents the central value of the range of reported f_s measurements [11,12], and the uncertainty has been chosen to cover half of the difference between the minimum and maximum values. It is also consistent with the suppression of strange hadrons observed in the production of light quark hadrons [25]. With these values for the fragmentation fractions, we determine

$$\mathcal{B}(B_s^0 \to J/\psi\phi) = (0.93 \pm 0.28 \pm 0.10 \pm 0.14) \times 10^{-3}. \tag{15}$$

The first uncertainty is statistical, the second accounts for the systematic uncertainties associated with the ratio of branching fraction measurements and the third is the uncertainty associated with the value we have taken for f_s.

We can also use these data to improve our knowledge of the branching fractions $\mathcal{B}(B^+ \to J/\psi K^+)$, $\mathcal{B}(B^0 \to J/\psi K^0)$, $\mathcal{B}(B^+ \to J/\psi K^{*+})$ and $\mathcal{B}(B^0 \to J/\psi K^{*0})$ using the world average values for the branching fractions, our ratios of branching fractions and the assumption that $f_u = f_d$. For example, for the decay $B^+ \to J/\psi K^{*+}$, we have three separate estimates

$$\mathcal{B}(B^+ \to J/\psi K^{*+}) = \mathcal{B}(B^+ \to J/\psi K^+) R_{K^+}^{K^{*+}}, \tag{16}$$

$$\mathcal{B}(B^+ \to J/\psi K^{*+}) = \mathcal{B}(B^0 \to J/\psi K^0) \left(\frac{f_d}{f_u}\right) R_{K^0}^{K^{*+}}, \text{ and} \tag{17}$$

$$\mathcal{B}(B^+ \to J/\psi K^{*+}) = \mathcal{B}(B^0 \to J/\psi K^{*0}) \left(\frac{f_d}{f_u}\right) \frac{1}{R_{K^{*+}}^{K^{*0}}}. \tag{18}$$

We use for the first term on the right-hand side of these estimates the world average values for the branching fractions [13] and form the weighted average of these three measurements, thereby reducing the statistical uncertainties. Because we employ in this calculation the world averages that have been determined assuming that $f_u = f_d$, these results depend implicitly on this assumption.

Using this procedure, we obtain the branching fractions

$$\mathcal{B}(B^+ \to J/\psi K^+) = (0.82 \pm 0.18 \pm 0.07) \times 10^{-3} \tag{19}$$

$$\mathcal{B}(B^0 \to J/\psi K^0) = (1.14 \pm 0.27 \pm 0.09) \times 10^{-3} \tag{20}$$

$$\mathcal{B}(B^+ \to J/\psi K^{*+}) = (1.73 \pm 0.55 \pm 0.15) \times 10^{-3} \tag{21}$$

$$\mathcal{B}(B^0 \to J/\psi K^{*0}) = (1.39 \pm 0.32 \pm 0.11) \times 10^{-3}, \tag{22}$$

where the first and second uncertainties are the statistical and systematic uncertainties, respectively. The statistical and systematic uncertainties have been estimated by weighting the relative contributions in the world average values and our data. The uncertainties in the world average branching fractions used in this calculation are dominated by the most recent measurements by the CLEO collaboration [22]. These uncertainties are limited by the size of the CLEO dataset, and are therefore largely statistical and independent. We have examined the stability of these estimates to different assumptions concerning the independence of the quoted systematic uncertainties. We find that our results and their estimated uncertainties are insensitive to possible correlations in the systematic uncertainties in the CLEO measurements.

We have compared our results with a calculation of the two-body nonleptonic decays of B mesons, using the factorization hypothesis, chiral and heavy quark symmetries and data from semileptonic D-decays [3]. We corrected the predicted ratios by the measured B meson lifetimes [13] to correct for the observed lifetime differences of these three states. Although several recent theoretical calculations of these branching fractions exist, we have selected Ref. [3] for this comparison as it predicts the branching fractions for the five decays studied here. The other model calculations have been made with varying theoretical assumptions and observational constraints, but they generally predict ratios of branching fractions that are in reasonable agreement with each other and our observations. It should be noted that these calculations generally assume the validity of factorisation as applied to non-leptonic B meson decays but they differ in many details, such as the magnitude and shape of the form factors for B meson decay and the experimental constraints employed in the calculations. In Ref. [3], the form factors are normalised to D meson semileptonic decay data and are assumed to be consistent with simple pole dominance. This assumption has been criticised recently [23,24] in the light of data on the observed polarisation in the decay $B \to J/\psi K^*$.

The results of the comparisons are shown in Fig. 5. In order to compare ratios involving B_s^0 decays, we have assumed $f_u = f_d$ and $f_s = (0.40 \pm 0.06)\ f_u$. The predictions agree well with the observed ratios of branching fractions, including the relative magnitude of the ratios involving B_s^0 meson decays as well as the ratios involving only B^+ and B^0 meson decays. The generally good agreement between data and prediction support the theoretical approach.

B. Ratios of Meson Fragmentation Fractions

The b quark fragmentation fractions have not been directly measured in a hadron collider environment. Our data allow us to constrain the ratios of these fractions. However, we note that the measured branching fractions of the B^+ and B^0 mesons have been determined assuming equal fragmentation fractions of b quarks produced in $\Upsilon(4S)$ decays. We therefore cannot employ the world average values for these quantities in estimating f_u, f_d or f_s.

Expressed in terms of fragmentation and branching fractions, the two ratios $R_{K^+}^{K^0}$ and $R_{K^{*+}}^{K^{*0}}$ give the relations

$$\frac{f_d}{f_u} = R_{K^+}^{K^0} \frac{\mathcal{B}(B^0 \to J/\psi K^+)}{\mathcal{B}(B^+ \to J/\psi K^0)}, \tag{23}$$

$$\frac{f_d}{f_u} = R_{K^{*+}}^{K^{*0}} \frac{\mathcal{B}(B^0 \to J/\psi K^{*+})}{\mathcal{B}(B^+ \to J/\psi K^{*0})}. \tag{24}$$

Under the assumption that these ratios of branching fractions are unity (which is the result of most quark model predictions), the weighted average of these two quantities gives

$$\frac{f_d}{f_u} = 0.99 \pm 0.19 \pm 0.08. \tag{25}$$

This result is consistent with the hypothesis that b quarks hadronise equally often into B^+ and B^0 mesons.

The strange meson fragmentation fraction f_s is constrained by the ratios that involve the B_s^0 final state, yielding the relationships

$$\frac{f_s}{f_u} = R^{\phi}_{K^{*+}} \frac{\mathcal{B}(B^+ \to J/\psi K^{*+})}{\mathcal{B}(B_s^0 \to J/\psi\phi)}, \tag{26}$$

$$\frac{f_s}{f_d} = R^{\phi}_{K^{*0}} \frac{\mathcal{B}(B^+ \to J/\psi K^{*0})}{\mathcal{B}(B_s^0 \to J/\psi\phi)}, \tag{27}$$

$$\frac{f_s}{f_u} = R^{\phi}_{K^{+}} \frac{\mathcal{B}(B^+ \to J/\psi K^{+})}{\mathcal{B}(B_s^0 \to J/\psi\phi)}, \tag{28}$$

$$\frac{f_s}{f_d} = R^{\phi}_{K^{0}} \frac{\mathcal{B}(B^+ \to J/\psi K^{0})}{\mathcal{B}(B_s^0 \to J/\psi\phi)}. \tag{29}$$

If we assume equal B^+ and B^0 decay rates to the $J/\psi K^*$ final states, equal B^+ and B^0 decay rates to the $J/\psi K$ final states and $f_u = f_d$, we obtain the ratios

$$\frac{f_s}{(f_u, f_d)} = (0.24 \pm 0.07 \pm 0.02) \frac{\mathcal{B}(B \to J/\psi K^*)}{\mathcal{B}(B_s^0 \to J/\psi\phi)} \text{ and} \tag{30}$$

$$\frac{f_s}{(f_u, f_d)} = (0.39 \pm 0.11 \pm 0.04) \frac{\mathcal{B}(B \to J/\psi K)}{\mathcal{B}(B_s^0 \to J/\psi\phi)}. \tag{31}$$

The hadronization probability of B_s^0 mesons inferred from these data depends on the ratios of branching fractions in Eq. (30) and (31). We take for the ratios of these fractions the values predicted in [3] and correct for lifetime differences as discussed earlier. We find that

$$\frac{f_s}{(f_u, f_d)} = 0.34 \pm 0.10 \pm 0.03. \tag{32}$$

C. Absolute Fragmentation Fractions

The hadronisation of b quarks produces both B mesons and baryons. Most B hadron decay models predict that virtually all B hadrons produced during the fragmentation process will subsequently decay via modes that include a ground state B meson or Λ_b^0 baryon. A measurement of the rate of Λ_b^0 production in b quark fragmentation gives us a direct measure of f_{Λ_b}, the probability that a bottom quark will hadronise such that a Λ_b^0 baryon is produced. This combined with our measurements of the ratios of fragmentation fractions allows us to make the first reported measurement of the values of f_u, f_d and f_s.

Studies of Λ_c^+ production in semileptonic b quark decays [27–29] have yielded measurements of the product

$$f_{\Lambda_b}\mathcal{B}(\Lambda_b^0 \to \Lambda_c^+\ell^-\bar{\nu}_\ell X). \tag{33}$$

The näive spectator quark model would predict that the inclusive Λ_b^0 semileptonic branching fraction to a final state with a charm hadron X_c is in the range of 0.10. A more detailed theoretical calculation [30] suggests a possible range of $0.10 - 0.13$. We have therefore chosen to use the inclusive branching fraction $\mathcal{B}(\Lambda_b^0 \to X_c\ell^-\bar{\nu}_\ell) = 0.115$, the central value of the theoretical prediction to estimate f_{Λ_b}. Assuming this value and the three most recent measurements of Λ_b^0 production in b quark fragmentation, we find that $f_{\Lambda_b} = 0.096 \pm 0.017$. It is of interest to note that the observed ratio of meson to baryon production [25] in minimum bias $p\bar{p}$ collisions at $\sqrt{s} = 630$ GeV, 6.4 ± 1.1, yields a baryon production fraction of 0.14 ± 0.02. This is consistent with the value determined from Λ_b^0 semileptonic decays even though these two fractions are not necessarily expected to be equal.

Using the condition that the fragmentation fractions should sum to unity, and assuming that the fraction of charm B hadrons $f_c \ll 1$, then

$$f_u + f_d + f_s + f_{\Lambda_b} = 1. \tag{34}$$

This can be rearranged to determine values for f_u, f_d and f_s using f_{Λ_b} and our measured ratios of fragmentation fractions:

$$f_u = \frac{1 - f_{\Lambda_b}}{1 + \frac{f_d}{f_u} + \frac{f_s}{f_u}} \tag{35}$$

$$f_d = \frac{1 - f_{\Lambda_b}}{1 + \frac{f_u}{f_d} + \frac{f_s}{f_d}} \tag{36}$$

$$f_s = \frac{1 - f_{\Lambda_b}}{1 + \frac{f_d}{f_s} + \frac{f_u}{f_s}} \tag{37}$$

$$\tag{38}$$

We find that $f_u = 0.39 \pm 0.04 \pm 0.04$, $f_d = 0.38 \pm 0.04 \pm 0.04$ and $f_s = 0.13 \pm 0.03 \pm 0.01$.

In phenomenological fragmentation models, the probabilities f_u, f_d and f_s are related to the relative probabilities of producing a $u\bar{u}$, $d\bar{d}$ and $s\bar{s}$ quark pair in the quark fragmentation process [26]. Measurements of the relative probabilities of strange meson to light meson production in e^+e^- and hadron-hadron collisions [11] and in deep inelastic scattering have yielded values in the range of 0.3 to 0.4. A recent compilation of these data has yielded a value of 0.29 ± 0.015 for the relative rate of strange quark production to up or down quark production [25], which agrees well with our values measured in b quark fragmentation. Taken together, these measurements indicate that the rate of $s\bar{s}$ suppression in quark fragmentation is largely independent of energy and flavour of the quark initiating the fragmentation process.

VI. CONCLUSION

We have used these data to determine the relative branching fractions of the B mesons into the observed final states. We have made the first measurement of a B_s^0 branching fraction to a final state with a J/ψ meson, yielding

$$\mathcal{B}(B_s^0 \to J/\psi\phi) = (0.93 \pm 0.28 \pm 0.10 \pm 0.14) \times 10^{-3}, \tag{39}$$

where we have assumed that $f_u = f_d$ and $f_s = (0.40 \pm 0.06) f_u$. We have also used our data in conjuction with the world average branching fractions to find

$$\mathcal{B}(B^+ \to J/\psi K^+) = (0.82 \pm 0.18 \pm 0.07) \times 10^{-3} \tag{40}$$

$$\mathcal{B}(B^0 \to J/\psi K^0) = (1.14 \pm 0.27 \pm 0.09) \times 10^{-3} \tag{41}$$

$$\mathcal{B}(B^+ \to J/\psi K^{*+}) = (1.73 \pm 0.55 \pm 0.15) \times 10^{-3} \tag{42}$$

$$\mathcal{B}(B^0 \to J/\psi K^{*0}) = (1.39 \pm 0.32 \pm 0.11) \times 10^{-3}, \tag{43}$$

where we have assumed $f_u = f_d$. These data are consistent with a B_s^0 branching fraction approximately equal to the B^+ and B^0 decays into topologically similar final states and a B_s^0 fragmentation fraction that is $\sim 30\%$ that of the B^+ or B^0 mesons.

The observed branching fractions are in good agreement with model calculations employing factorization and chiral and heavy quark symmetries.

An analysis of the ratios of branching fractions confirms the widely-held assumption that the probabilities of producing B^+ and B^0 mesons in b quark fragmentation are equal. We measured the ratio of f_d to f_u to be $0.99 \pm 0.19 \pm 0.08$. If we assume the theoretically predicted ratios of branching fractions for the $B_s^0 \to J/\psi\phi$ relative to topologically similar decay modes for the B^+ and B^0 mesons and we assume $f_u = f_d$, we determine that $f_s/(f_u, f_d) = 0.34 \pm 0.10 \pm 0.03$. Employing an estimate for the fraction of Λ_b^0 production in b quark fragmentation, $f_{\Lambda_b} = 0.096 \pm 0.017$, we determine $f_u = 0.39 \pm 0.04 \pm 0.04$, $f_d = 0.38 \pm 0.04 \pm 0.04$ and $f_s = 0.13 \pm 0.03 \pm 0.01$. These measurements imply a suppression of $s\bar{s}$ production relative to $u\bar{u}$ and $d\bar{d}$ production in b quark fragmentation similar to that measured in e^+e^- and deep inelastic scattering experiments.

Our measurements are limited by the number of fully reconstructed B mesons in our sample. A data sample approximately four times larger than the one used in this study is under preparation, which will allow us to significantly reduce the statistical uncertainties in these ratios.

VII. ACKNOWLEDGEMENTS

We thank the Fermilab staff and the technical staff at the participating institutions for their essential contributions to this research. This work is supported by the U. S. Department of Energy and the National Science Foundation; the Natural Sciences and Engineering Research Council of Canada; the Istituto Nazionale di Fisica Nucleare of Italy; the Ministry of Education, Science and Culture of Japan; the National Science Council of the Republic of China; and the A. P. Sloan Foundation.

REFERENCES

[1] S. L. Glashow, Nucl. Phys. **22**, 579 (1961);

S. Weinberg, Phys. Rev. Lett. **19**, 1264 (1967);

A. Salam, "Elementary Particle Theory," ed. N. Svartholm, Almquist and Wiksells, Stockholm, 367 (1969).

[2] M. Wirbel, B. Stech and M. Bauer, Z. Phys. C **29**, 637 (1985); M. Bauer, B. Stech and M. Wirbel, Z. Phys. C **34**, 103 (1987).

[3] A. Deandrea, N. Di Bartolomeo, R. Gatto and G. Nardulli, Phys. Lett. B **318**, 549 (1993).

[4] G. Kramer and W. Palmer, Phys. Rev. D **46**, 2969 (1992);

G. Kramer and W. Palmer, Phys. Rev. D **46**, 3197 (1992).

[5] M. S. Alam *et al.* (CLEO Collaboration), Phys. Rev. D **50**, 43 (1994).

[6] H. Albrecht *et al.* (ARGUS Collaboration), Phys. Lett. B **185**, 218 (1987); Phys. Lett. B **215**, 424 (1988); Z. Phys. C. **48**, 543 (1990).

[7] F. Abe *et al.* (CDF Collaboration), Phys. Rev. D. **53**, 1051 (1996).

[8] S. Abachi *et al.* (D0 Collaboration), Phys. Rev. Lett. **74**, 3548 (1995).

[9] F. Abe *et al.* (CDF Collaboration), Phys. Rev. Lett. **75**, 1451 (1995).

[10] F. Abe *et al.* (CDF Collaboration), Phys. Rev. Lett. **76**, 2015 (1996).

[11] V. Ammosov *et al.*, Phys. Lett. **B93**, 210 (1980);

R. Brandelik *et al.* (TASSO Collaboration), Phys. Lett. B **117**, 135 (1982);

P. K. Malhotra and R. Orava, Phys. Lett. B **17**, 85 (1983);

W. Bartel *et al.* (JADE Collaboration), Z. Phys. C. **20**, 187 (1983);

H. Aihara *et al.* (PEP-4 Collaboration), Phys. Rev. Lett. **53**, 2378 (1984);

G. J. Alner *et al.*, Nucl. Phys. **B258**, 505 (1985);

R. E. Ansorge *et al.*, Z. Phys. C **41**, 179 (1988);

D. Bortoletto *et al.* (CLEO Collaboration), Phys. Rev. D **37**, 1719 (1988);

F. Abe *et al.* (CDF Collaboration), Phys. Rev. D **40**, 3791 (1989).

[12] P. Abreu *et al.* (DELPHI Collaboration), Z. Phys. C. **61**, 407 (1994).

[13] Particle Data Group, M. Aguilar-Benitez *et al.*, Phys. Rev. D **37**, 1 (1994).

[14] We employ a coordinate system where the $\hat{z}$ axis is along the proton beam direction, θ is the polar angle relative to $\hat{z}$ and ϕ is the azimuthal angle. Pseudorapidity is defined as $\eta \equiv \ln\tan(\theta/2)$.

[15] F. Abe *et al.* (CDF Collaboration), Nucl. Instrum. Methods Phys. Res., Sect. A **271**, 387 (1988); D. Amidei *et al.*, Nucl. Instrum. Methods Phys. Res., Sect. A **350**, 73 (1994). F. Abe *et al.* (CDF Collaboration), Phys. Rev. D **52**, 4784 (1995).

[16] S. Dawson *et al.*, Nucl. Phys. B **327**, 49 (1988); M. Mangano *et al.*, Nucl. Phys. B **373**, 295 (1992).

[17] A. D. Martin, W. J. Stirling and R. G. Roberts, Phys. Rev. D **47**, 467 (1993).

[18] C. Peterson, D. Schlatter, I. Schmitt and P. Z. Zerwas, Phys. Rev. D **27**, 105 (1983).

[19] P. Avery, K. Read and G. Trahern, Cornell Internal Note CSN-212, Mar. 1985 (unpublished).

[20] F. Abe *et al.* (CDF Collaboration), Phys. Rev. Lett. **75**, 3068 (1995).

[21] T. Sjöstrand, Computer Physics Commun. **82**, 74 (1994). PYTHIA Version 5.7 was used.

[22] M. S. Alam *et al.* (CLEO Collaboration), Phys. Rev. D **50**, 43 (1994). CLEO B paper.

[23] M. Gourdin, A. N. Kamal and X. Y. Pham, Phys. Rev. Lett. **73**, 3355 (1994).

[24] R. Aleksan, A. Le Yaouanc, L. Oliver, O. Pene and J.-C. Raynal, Phys. Rev. D **51**,

6235 (1995).

[25] G. Bocquet *et al.*, Phys. Lett. B **366**, 447 (1996).

[26] V. V. Anisovich and V. M. Shekhter, Nucl. Phys. B **55**, 455 (1973);
R. D. Field and R. P. Feynman, Nucl. Phys. B **136**, 1 (1978);
B. Andersson *et al.*, Z. Phys. C **20**, 317 (1983).

[27] P. Abreu *et al.* (DELPHI Collaboration), Z. Phys. C **68**, 375 (1995).

[28] D. Buskulic *et al.* (ALEPH Collaboration), Phys. Lett. B **357**, 685 (1995).

[29] R. Akers *et al.* (OPAL Collaboration), Z. Phys. C **69**, 195 (1996).

[30] T. Mannel and G. A. Schuler, Phys. Lett. B **279**, 194 (1992).

FIGURES

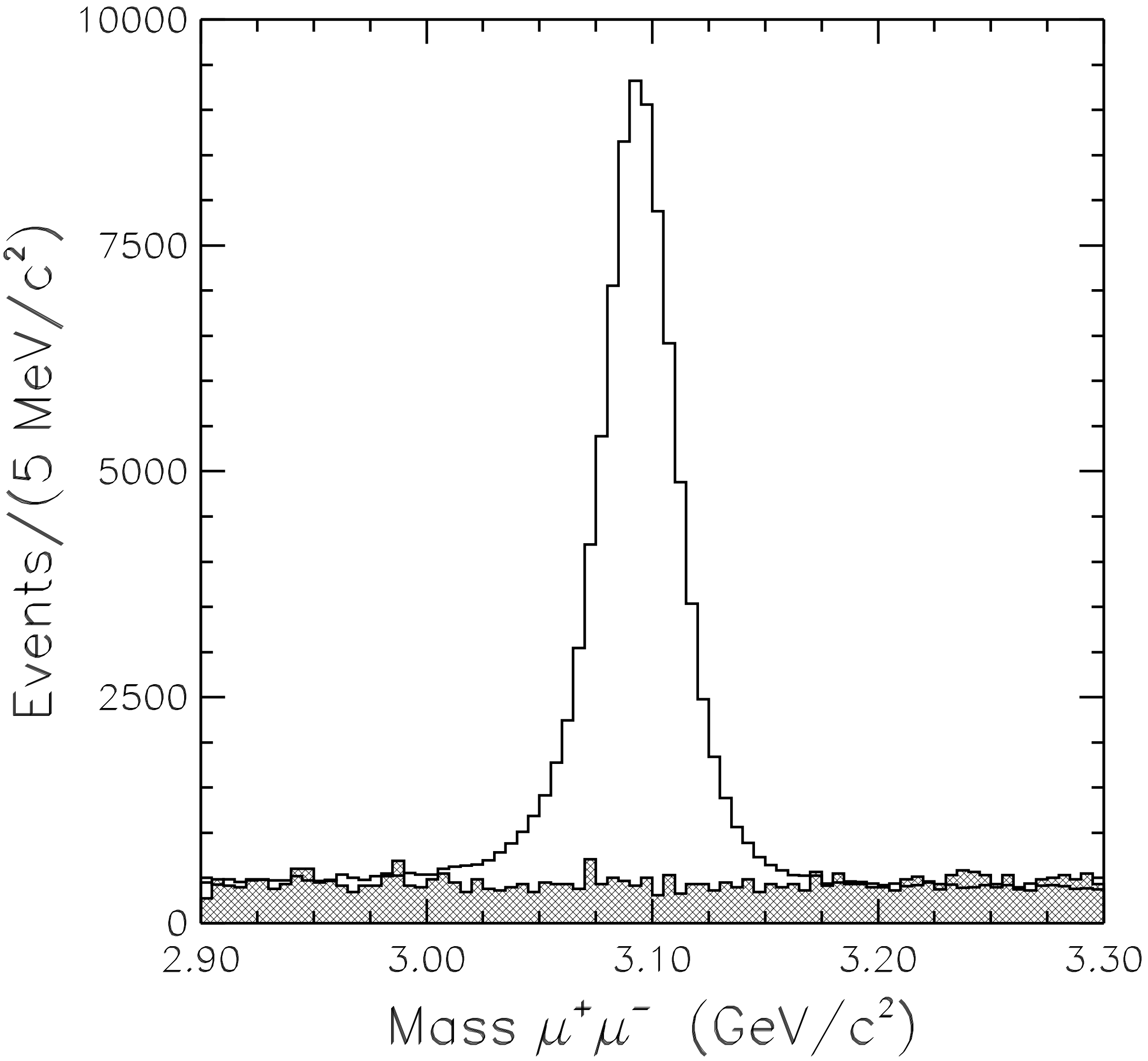

FIG. 1. The dimuon invariant mass distribution for the inclusive J/ψ event sample. The shaded distribution is for same-sign dimuon candidates.

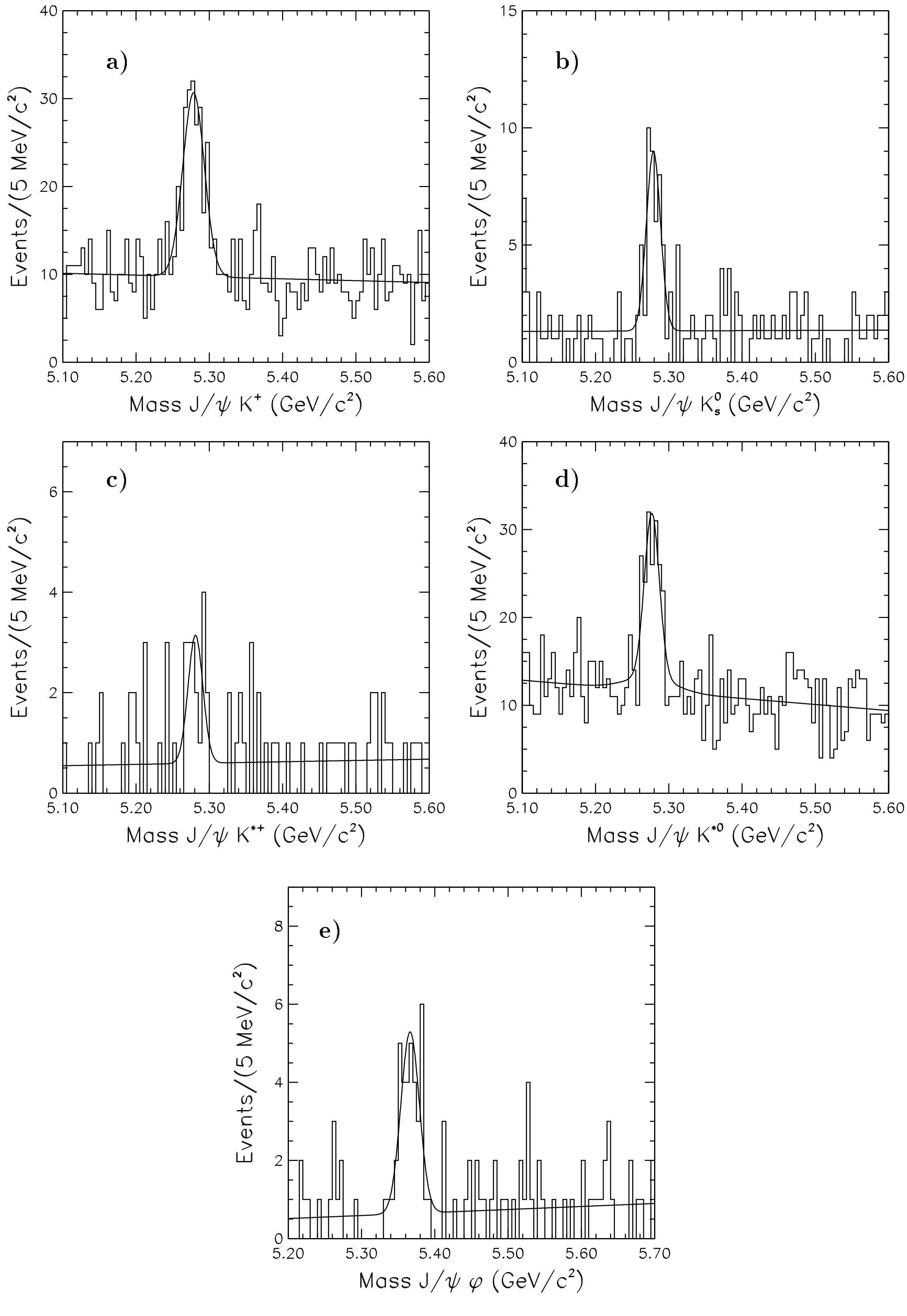

FIG. 2. The $J/\psi K^+$ invariant mass distribution is shown in a). The invariant mass distributions for the $J/\psi K_s^0$, $J/\psi K^{*+}$, $J/\psi K^{*0}$ and $J/\psi \phi$ candidate events are shown in b) through e), respectively.

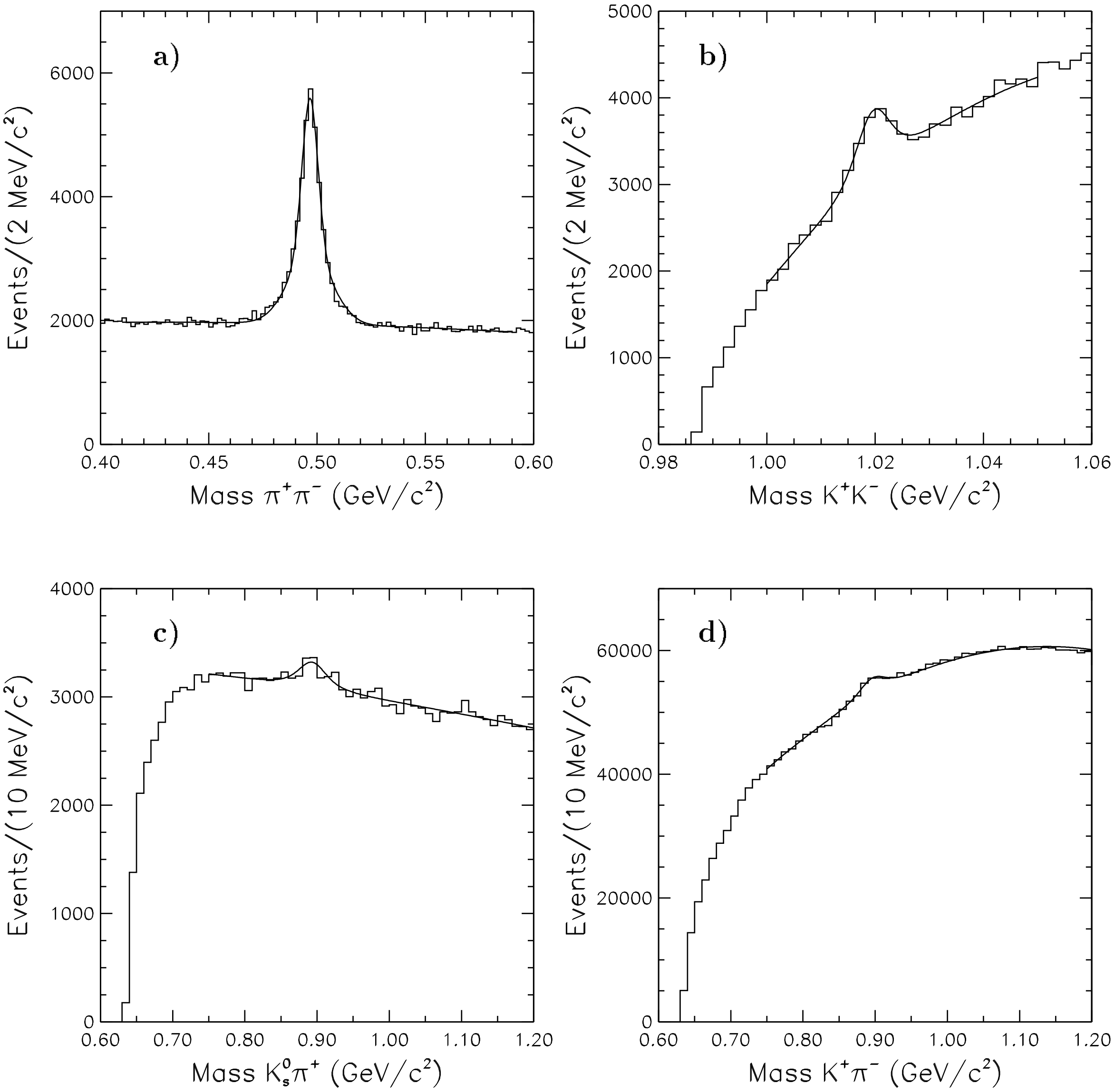

FIG. 3. The $\pi^+\pi^-$ invariant mass distribution is shown in a) for K_s^0 candidates. The K^+K^- invariant mass distribution is shown in b). The $K_s^0\pi^+$ invariant mass distribution is shown in c) for events that have satisfactory fits to the $K_s^0\pi^+$ hypothesis. The $K^+\pi^-$ invariant mass distribution is shown in d).

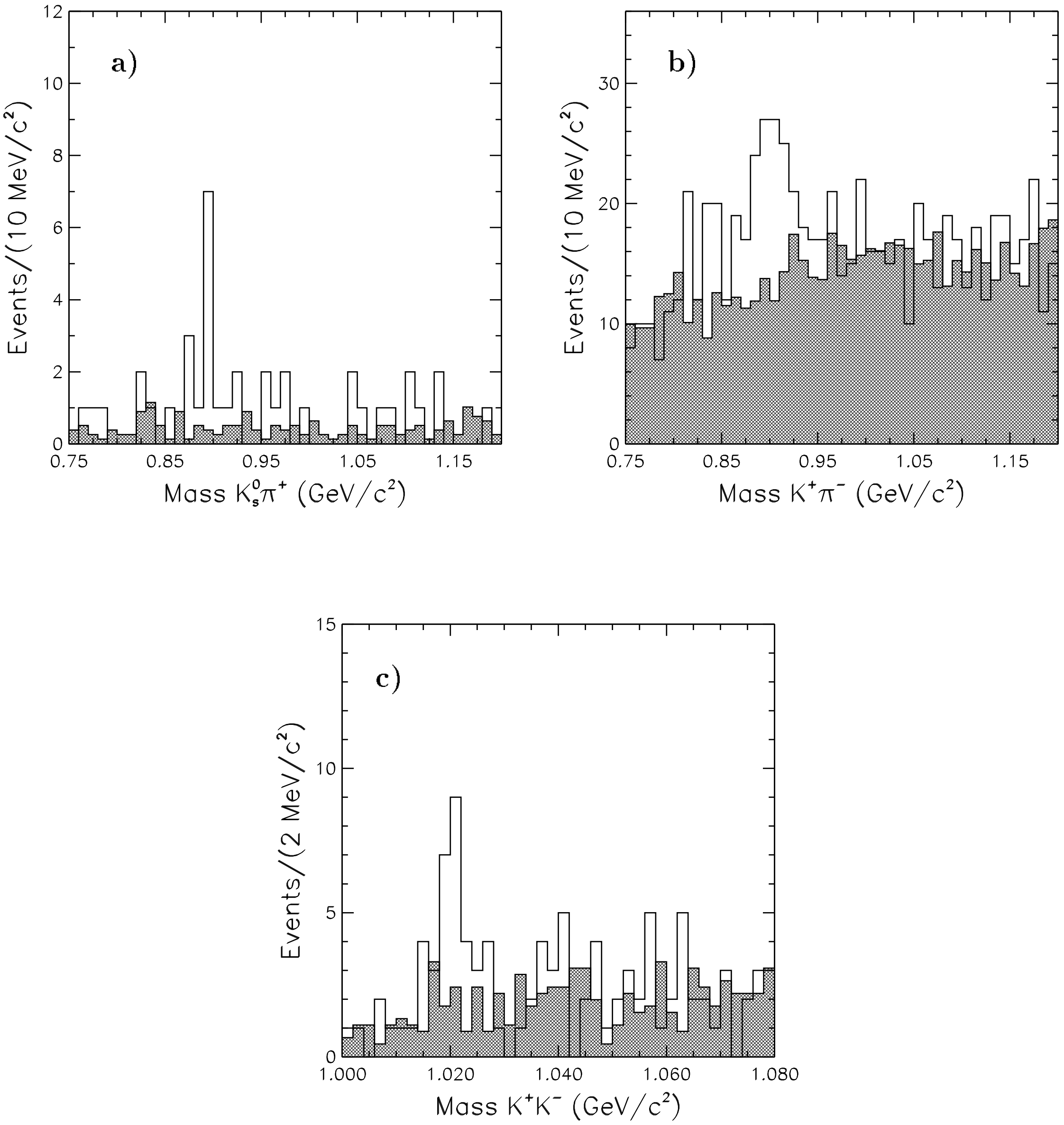

FIG. 4. The $K_s^0\pi^+$ invariant mass distributions for the B^+ signal and sideband regions are shown in a). The B^+ signal region is represented by the unshaded histogram. The B^+ sideband region, normalised to the non-B^+ background in the B^+ signal region, is the shaded distribution. The corresponding distributions for the $K^+\pi^-$ and K^+K^- invariant mass are shown in b) and c), respectively.

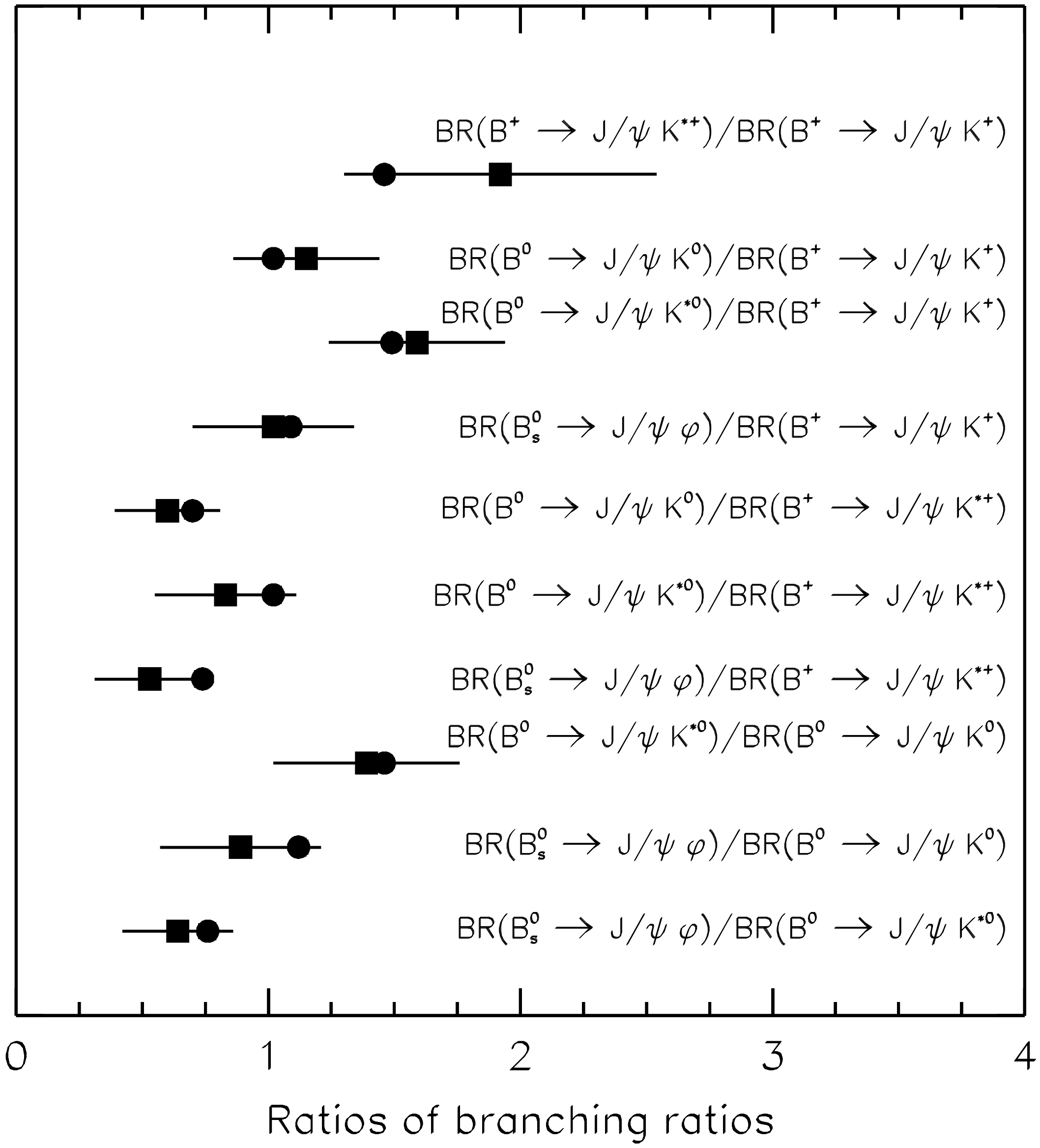

FIG. 5. Comparison of observed ratios of branching fractions (squares) with the theoretical prediction (circles) described in the text. The error bars reflect the statistical and systematic uncertainties of the observed ratios added in quadrature.

TABLES

TABLE I. The definition of the signal regions, sideband regions and the number of observed events associated with the decays $B^+ \to J/\psi K^{*+}$, $B^0 \to J/\psi K^{*0}$ and $B_s^0 \to J/\psi\phi$. The number of observed events is calculated in three ways: fitting the resonant structure in the $K\pi$ and KK invariant mass distributions either using the sideband distributions to estimate the background (N_{sb}) or using a second order polynomial to estimate the background (N_{fit}), and using the number of observed B candidate events, correcting for the loss of resonant decays due to the two-body mass requirement (N_{win}). The number of events obtained using the sideband subtracted background, N_{sb}, is used to calculate the branching fraction ratios.

	$J/\psi K_s^0\pi^+$	$J/\psi K^+\pi^-$	$J/\psi K^+K^-$
Signal Region (GeV/c^2)	5.235-5.325	5.235-5.325	5.320-5.410
Sideband Regions (GeV/c^2)	5.000-5.220	5.000-5.180	5.100-5.305
	5.340-5.600	5.380-5.600	5.425-5.700
N_{sb} (events)	21.3 ± 6.1	119 ± 20	26.7 ± 7.3
N_{fit} (events)	17.0 ± 6.5	108 ± 27	27.3 ± 7.4
N_{win} (events)	16.0 ± 5.3	119 ± 18	34.4 ± 7.3

TABLE II. The number of observed signal events and the reconstruction efficiencies for the five decay modes. The geometrical efficiency includes the meson P_T requirements and the acceptance of the tracking fiducial volume. It does not include the J/ψ or meson branching fractions. The efficiencies of the B proper decay length requirement and the reconstruction efficiencies of the light quark mesons are also listed.

Channel	Events	ϵ_{geom}	$\epsilon_{c\tau}$	ϵ_{meson}
$B^+ \to J/\psi K^\pm$	154 ± 19	$(10.1 \pm 0.6) \times 10^{-2}$	0.900 ± 0.005	0.979 ± 0.007
$B^0 \to J/\psi K^0$	36.9 ± 7.3	$(7.95 \pm 0.54) \times 10^{-2}$	0.876 ± 0.007	0.857 ± 0.011
$B^+ \to J/\psi K^{*\pm}$	21.3 ± 6.1	$(3.41 \pm 0.26) \times 10^{-2}$	0.880 ± 0.006	0.839 ± 0.013
$B^0 \to J/\psi K^{*0}$	119 ± 20	$(6.85 \pm 0.45) \times 10^{-2}$	0.893 ± 0.006	0.958 ± 0.010
$B_s^0 \to J/\psi \phi$	26.7 ± 7.3	$(10.7 \pm 0.7) \times 10^{-2}$	0.884 ± 0.020	0.904 ± 0.021

TABLE III. The systematic uncertainties in the relative efficiencies for the different channels.

Effect	Systematic Uncertainty (%)
B meson geometrical efficiency	1
Detector simulation	5
$K^\pm$ reconstruction efficiency	1
Vector meson polarization	2.5
K_s^0 reconstruction	1
B P_T Spectrum	1-5
Effects of Resonant B Production	1-4

TABLE IV. The ratio of fragmentation fractions and branching fractions for the various B meson final states. The ratio R_i^j is located in the ith row and jth column.

	$(J/\psi K^0)$	$(J/\psi K^{*+})$	$(J/\psi K^{*0})$	$(J/\psi \phi)$
$(J/\psi K^+)$	$1.15 \pm 0.27 \pm 0.09$	$1.92 \pm 0.60 \pm 0.17$	$1.59 \pm 0.33 \pm 0.12$	$0.41 \pm 0.12 \pm 0.04$
$(J/\psi K^0)$		$1.68 \pm 0.58 \pm 0.11$	$1.39 \pm 0.36 \pm 0.10$	$0.35 \pm 0.12 \pm 0.03$
$(J/\psi K^{*+})$			$0.83 \pm 0.27 \pm 0.06$	$0.21 \pm 0.08 \pm 0.02$
$(J/\psi K^{*0})$				$0.26 \pm 0.08 \pm 0.02$